PHYSICAL REVIEW D **87,** 125034 (2013)

Sterile neutrinos: Cosmology versus short-baseline experiments

Maria Archidiacono,[1] Nicolao Fornengo,[2] Carlo Giunti,[2] Steen Hannestad,[1] and Alessandro Melchiorri[3]
[1]*Department of Physics and Astronomy, Aarhus University, 8000 Aarhus C, Denmark*
[2]*Department of Physics, University of Torino and INFN, Via P. Giuria 1, I-10125 Torino, Italy*
[3]*Physics Department, Università di Roma "La Sapienza" and INFN, Ple Aldo Moro 2, 00185 Rome, Italy*
(Received 1 March 2013; published 27 June 2013)

Cosmology and short-baseline (SBL) neutrino oscillation data both hint at the existence of light sterile neutrinos with masses in the 1 eV range. Here we perform a detailed analysis of the sterile neutrino scenario using both cosmological and SBL data. We have additionally considered the possibility that the extra neutrino degrees of freedom are not fully thermalized in the early universe. Even when analyzing only cosmological data we find a preference for the existence of massive sterile neutrinos in both $(3 + 1)$ and $(3 + 2)$ scenarios, and with the inclusion of SBL data the evidence is formally at the 3.3σ level in the case of a $(3 + 1)$ model. Interestingly, cosmological and SBL data both point to the same mass scale of approximately 1 eV. In the $(3 + 1)$ framework WMAP9 + SPT provide a value of the sterile mass eigenstate $m_4 = (1.72 \pm 0.65)$ eV; this result is strengthened by adding the prior from SBL posterior to $m_4 = (1.27 \pm 0.12)$ eV [$m_4 = (1.23 \pm 0.13)$ eV when data from the Sloan Digital Sky Survey is also considered in the cosmological analysis]. In the $(3 + 2)$ scheme, two additional, nonfully thermalized neutrinos are compatible with the whole set of cosmological and SBL data, leading to mass values of $m_4 = (0.95 \pm 0.30)$ eV and $m_5 = (1.59 \pm 0.49)$ eV. The inclusion of Planck data does not change our considerations about the mass scale; concerning the extra neutrino degrees of freedom, by invoking a partial thermalization the $3 + 1$ model is still consistent with the latest data.

DOI: 10.1103/PhysRevD.87.125034 PACS numbers: 14.60.Pq, 14.60.St, 98.80.−k, 98.80.Es

I. INTRODUCTION

The past decade has seen a rapid increase in our understanding of neutrinos. Oscillation experiments have now established the main structure of the leptonic mixing matrix and provided evidence for at least two neutrino mass states of nonzero mass (see e.g. Ref. [1] for a recent overview). However, some crucial questions are still left unanswered: the absolute mass scale of neutrinos is extremely hard to measure in laboratory experiments and is therefore currently only poorly known; the hierarchy of neutrino masses is not yet disentangled; the possible existence of additional neutrino species beyond the three predicted by the Standard Model is still an open issue. In fact, short-baseline (SBL) oscillation experiments, as well as reactor neutrino flux measurements seem to hint at the existence of a fourth ($3 + 1$ models, possibly with nonstandard interactions) or fifth ($3 + 2$ models) sterile neutrino, with the active neutrinos and with a mass around 1 eV, see Refs. [2–7].

Cosmology has, at the same time, provided important insights into some of these questions. Neutrinos are produced in copious amounts in the early Universe, and are still present as a cosmic neutrino background. Even though this background is extremely difficult if not impossible to measure directly, it influences a number of cosmological observables such as the cosmic microwave background (CMB), and the power spectrum of matter fluctuations. The effective number of relativistic degrees of freedom changes both the position and the shape of peaks of the CMB temperature power spectrum at high multipoles [8]. The neutrino mass affects both the CMB, through the enhancement of the early integrated Sachs-Wolfe effect, and the matter power spectrum, via the free-streaming that suppresses the power on small scales. Thanks to these fingerprints, cosmology can strongly constrain the absolute neutrino mass scale and the cosmic neutrino background [9,10].

In the past years cosmology has provided some hints for a nonstandard value of the effective number of relativistic degrees of freedom (see Refs. [11–14]), with the preferred value in the late-time Universe (around, or subsequent to, recombination) being significantly higher than the Standard Model prediction of $N_{\rm eff} = 3.046$ [15]. Such additional relativistic energy density is usually referred to as dark radiation and can arise from a completely different physics such as axions [16]. The light sterile neutrinos hinted at by SBL data would be an excellent candidate for dark radiation [17], even though misinterpretations of the nature of this nonstandard $N_{\rm eff}$ can arise from degeneracies between $N_{\rm eff}$ and other cosmological parameters [18].

Recently, new CMB data released by the WMAP collaboration [19], the South Pole Telescope (SPT) [20], and the Atacama Cosmology Telescope (ACT) [21] have led to a somewhat confusing situation concerning dark radiation and, in general, those neutrino properties that can be constrained by cosmology: the WMAP9 and SPT data both confirm the presence of an extra dark radiation component, while the new ACT data seem to point towards a value of $N_{\rm eff}$ in agreement with the Standard Model prediction, in contrast with their own previous analysis [22].

Fortunately this problem might be resolved by new data from the Planck mission [23] which should be able to constrain $N_{\rm eff}$ with a much better precision than existing data (see e.g. Refs. [24,25]). However, even if the incoming cosmological data from Planck confirms the standard cosmological value for $N_{\rm eff}$, cosmology should address the discrepancy with the SBL neutrino oscillation results. Since the SBL experiments do not provide a direct constraint on the cosmological thermalization of the sterile neutrinos, a small lepton asymmetry can be invoked to reduce the thermalization efficiency (see e.g. Refs. [26,27] for recent treatments) and reconcile these two branches of neutrino physics.

So it is indeed timely to investigate the interplay between neutrino oscillation experiments and cosmology in determining the neutrino properties [28–32]. This paper is aimed at investigating the joint constraints on neutrino number and neutrino mass from these two different branches. The paper is organized as follows: in Sec. II we present the SBL analysis data, which includes updates on our previous analysis; in Sec. III we describe the cosmological data used in this work and the method we have applied to analyze them; in Sec. IV we provide an update of the cosmological constraints on sterile neutrinos; in Sec. V we perform the joint analysis by applying a short-baseline prior to the cosmological analysis. Section VI contains our conclusions. Finally in Sec. VII we have applied the same model of Sec. V A to the analysis of Planck data [33] in order to check that the latest CMB measurements do not change our conclusions.

II. SBL ANALYSIS

We consider $3+1$ and $3+2$ extensions of the standard three-neutrino mixing (see Ref. [34]) in which we have one (m_4) or two (m_4 and m_5) new neutrino masses at the eV scale and the masses of the three standard neutrinos are much smaller,

$$m_1, m_2, m_3 \ll m_4 \leq m_5. \tag{1}$$

In this case, the squared-mass differences

$$\Delta m^2_{41} \simeq m^2_4 \quad \text{and} \quad \Delta m^2_{51} \simeq m^2_5, \tag{2}$$

with $\Delta m^2_{kj} \equiv m^2_k - m^2_j$, generate short-baseline oscillations through the mixing relation

$$\nu_\alpha = \sum_{k=1}^{4\ \text{or}\ 5} U_{\alpha k} \nu_k, \tag{3}$$

between the flavor neutrino fields ν_α ($\alpha = e, \mu, \tau, s_1, s_2$ in the $3+2$ model) and the neutrino fields ν_k with masses m_k ($k = 1, \ldots, 5$ in the $3+2$ model). U is the unitary mixing matrix.

In the analysis of short-baseline data we adopted the approach described in Ref. [28], with some improvements in the considered data sets, which can be divided into the following three groups:

(1) The $\nu_\mu \to \nu_e$ and $\bar{\nu}_\mu \to \bar{\nu}_e$ appearance data of the LSND [35], KARMEN [36], NOMAD [37], MiniBooNE [38], and ICARUS [39] experiments. In particular, we use only the MiniBooNE data above 475 MeV, because the data at lower energy contains an anomaly which cannot be explained by neutrino oscillations [4,5] (an interesting possibility of reconciling the low-energy anomalous data with neutrino oscillations through energy reconstruction effects has been suggested and discussed in Refs. [40,41]).

(2) The ν_e and $\bar{\nu}_e$ disappearance data described in Ref. [42], which take into account the reactor [43] and gallium [44] anomalies.

(3) The constraints on ν_μ and $\bar{\nu}_\mu$ disappearance obtained from the data of the CDHSW experiment [45], from the analysis [46] of the data of atmospheric neutrino oscillation experiments, from the analysis [4] of the MINOS neutral-current data [47], and from a new analysis of the SciBooNE-MiniBooNE neutrino [48] and antineutrino [49] data.

The results of a least-squares analysis of the SBL data is presented in Table I. First, we notice that the values of the goodness-of-fit obtained in the $3+1$ and $3+2$ models are satisfactory and much better than what is obtained in the case of the absence of sterile neutrinos ($3+0$). We notice also that the value of the appearance-disappearance parameter goodness-of-fit is acceptable and it is remarkable that it is better in the $3+1$ model than in the $3+2$ model, contrary to previous results with older data [2,3,50]. The reason is that the values of $\chi^2_{\rm min}$ for appearance (APP) and disappearance (DIS) data in the two models are

TABLE I. Values of $\chi^2_{\rm min}$, number of degrees of freedom (NDF), goodness-of-fit (GoF), and best-fit values of the mixing parameters obtained in our $3+0$, $3+1$, and $3+2$ fits of short-baseline oscillation data. The last three lines give the appearance-disappearance parameter goodness-of-fit (PG).

	$3+0$	$3+1$	$3+2$
$\chi^2_{\rm min}$	280.2	236.1	229.0
NDF	230	227	223
GoF (%)	1.3	32	38
Δm^2_{41} [eV^2]		1.62	0.91
$\lvert U_{e4}\rvert^2$		0.031	0.015
$\lvert U_{\mu 4}\rvert^2$		0.01	0.011
Δm^2_{51} [eV^2]			1.61
$\lvert U_{e5}\rvert^2$			0.0226
$\lvert U_{\mu 5}\rvert^2$			0.00664
η			1.56π
$\Delta\chi^2_{\rm PG}$		6.6	11.12
$\rm NDF_{PG}$		2	4
$\rm GoF_{PG}$		4%	2.5%

$$(\chi^2_{\rm min})^{3+1}_{\rm APP} = 50.4, \qquad (\chi^2_{\rm min})^{3+1}_{\rm DIS} = 179.1, \tag{4}$$

$$(\chi^2_{\rm min})^{3+2}_{\rm APP} = 40.1, \qquad (\chi^2_{\rm min})^{3+2}_{\rm DIS} = 177.8. \tag{5}$$

Since the 3 + 2 model can fit significantly better than the 3 + 1 model in only the appearance data, the larger difference between the global $\chi^2_{\rm min}$ and $(\chi^2_{\rm min})_{\rm APP} + (\chi^2_{\rm min})_{\rm DIS}$ in the 3 + 2 model cannot be compensated by the increase of the number of degrees of freedom.

Figure 1 shows the allowed 3σ regions (99.73% C.L.) in the $\sin^2 2\vartheta_{e\mu} - \Delta m^2_{41}$ plane in the 3 + 1 model obtained with disappearance data, appearance data, and all data respectively. The quantity $\sin^2 2\vartheta_{e\mu} = 4|U_{e4}|^2|U_{\mu 4}|^2$ is the amplitude of $\nu_\mu \to \nu_e$ and $\bar\nu_\mu \to \bar\nu_e$ oscillations (see Ref. [34]). One can see that the combination of the constraints obtained from disappearance data excludes the large-$\sin^2 2\vartheta_{e\mu}$ part of the regions allowed by appearance data. From the global fit we obtained a low-Δm^2_{41} allowed region at $\Delta m^2_{41} \simeq 0.8$–2 eV^2 and $\sin^2 2\vartheta_{e\mu} \simeq (0.5$–$3) \times 10^{-3}$, containing the best-fit point, and a high-Δm^2_{41} allowed region at $\Delta m^2_{41} \simeq 6$ eV^2 and $\sin^2 2\vartheta_{e\mu} \simeq (0.8$–$2) \times 10^{-3}$.

The appearance-disappearance tension discussed in previous papers (e.g. Refs. [2–5,50]) is still present, because, as one can see from Fig. 1, the best-fit point of the appearance data is excluded at about 3σ by the disappearance data. However, the tension is less severe than that which was obtained with old data, as testified by the acceptable parameter goodness-of-fit in Table I.

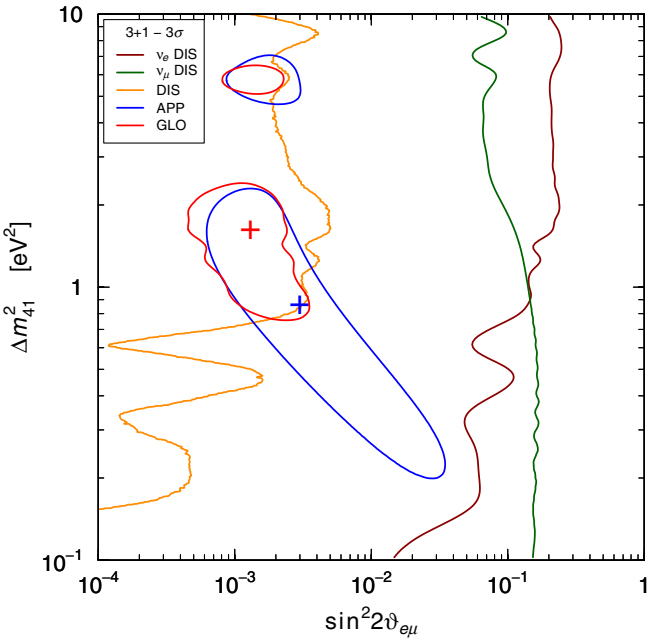

FIG. 1 (color online). Allowed 3σ regions (99.73% C.L.) in the $\sin^2 2\vartheta_{e\mu} - \Delta m^2_{41}$ plane in the 3 + 1 model obtained from ν_e and $\bar\nu_e$ disappearance data (left of the dark red curve), ν_μ and $\bar\nu_\mu$ disappearance data (left of the dark green curve), combined disappearance data (left of the dark orange curve), $\nu_\mu \to \nu_e$ and $\bar\nu_\mu \to \bar\nu_e$ appearance data (inside the blue curve), and from the global fit (inside the red curves). The best-fit points in the last two cases are indicated by crosses.

In the following we combine the results of the analysis of short-baseline and cosmological data considering both 3 + 1 and 3 + 2 schemes, in spite of the fact that the 3 + 1 scheme is sufficient to explain the current short-baseline data and the 3 + 2 scheme is disfavored by Occam's razor. We consider also the 3 + 2 scheme because of the current interest in it (see, for example, Ref. [51]) and because future data may reverse the preference.

III. COSMOLOGICAL METHOD

We have modified the Monte Carlo Markov Chain (MCMC) public package COSMOMC [52] (October 2012 version) to account for the data sets listed below and in order to sample the extended parameter space for our (3 + 1) and (3 + 2) investigations.

The cosmological analysis is performed by employing various combinations of data sets. The WMAP 9-year data release [19] represents our basic CMB data set. At high multipoles, we use new data from the CMB experiments South Pole Telescope [20] and Atacama Cosmology Telescope [21]. The information on dark matter clustering comes from the matter power spectrum derived from the Sloan Digital Sky Survey Data Release 7 luminous red galaxy sample [53]. We have also investigated the impact on our constraints of the Baryonic Acoustic Oscillations (BAO) results of Refs. [54–56] and of the prior on the Hubble constant coming from the Hubble Space Telescope measurements [57].

Short-baseline results have been included as a prior in the analysis. Therefore the final χ^2 of the combined analysis is simply given by

$$\chi^2_{\rm tot} = \chi^2_{\rm cosmology} + \chi^2_{\rm SBL}. \tag{6}$$

Concerning the inclusion of the SBL information in the cosmological analyses, the difference with respect to our previous work [28], is that here we directly incorporate the χ^2 coming from SBL data (analyzed in a variety of frameworks) in the MCMC sampling; this allows for unbiased constraints on those parameters that are common to the cosmological and SBL analyses.

Our basic cosmological model is the six-parameter flat ΛCDM model. Its parameters are the physical baryon and cold dark matter densities $\Omega_b h^2$ and $\Omega_{\rm dm} h^2$, the ratio of the sound horizon to the angular diameter distance at decoupling θ_s, the optical depth to reionization τ, the scalar spectral index n_s, and the overall normalization of the spectrum A_s. In the cosmological analyses, we also account for the Sunyaev-Zeldovich (SZ) effect and foreground contributions by including three extra amplitudes: the SZ amplitude $a_{\rm SZ}$, the amplitude of clustered point sources a_c, and the amplitude of Poisson distributed point sources a_p. Since the ACT team uses a different mask for identifying

and removing point sources, when the ACT data are included in our analysis (Sec. IV) a fourth extra amplitude is needed to account for the Poisson contribution in the ACT data $a_{p\mathrm{ACT}}$ different from $a_{p\mathrm{SPT}}$. Furthermore when the ACT likelihood is included in our analysis, we split the SZ contribution into two amplitudes to account for the two different SZ effects: $a_{k\mathrm{SZ}}$ for the kinetic SZ effect and $a_{t\mathrm{SZ}}$ for the thermal SZ effect.

In order to include extra sterile neutrinos, the ΛCDM model is extended to a Λ mixed dark matter model (ΛMDM) by introducing a hot dark matter component in the form of massive neutrinos. Usually this component is parametrized as the neutrino mass fraction f_ν (the neutrino-hot dark matter density over the total dark matter density), as in Sec. IV, but in the joint analysis of Sec. V the masses of the single mass eigenstate are used as free parameters, in order to directly sample the parameter which the SBL prior acts on.

With the above assumptions, the contribution of massive neutrinos to the energy budget of the Universe follows the usual relation,

$$\Omega_\nu h^2 = \frac{\sum m_\nu}{93.14\ \mathrm{eV}}, \tag{7}$$

where $\sum m_\nu$ denotes an effective sum of masses, specified below for the different cases under study.

Before attempting the combined (cosmological + SBL) analysis, we perform a number of tests on the cosmological data alone, in order to assess the requirements on dark radiation from the various cosmological data sets. These results will then be compared to the interpretation of dark radiation in terms of sterile neutrinos in the (3 + 1) and (3 + 2) models. From the point of view of cosmology there is no difference between active neutrinos and sterile neutrinos provided they are fully thermalized. For the typical mass differences and mixing angles hinted at by the SBL data this is indeed the case (see e.g. Refs. [26,27]). In this case only the total sum of neutrino masses and the total (effective) number of neutrino species are relevant parameters (with the current level of precision of cosmological data). However, it is entirely possible that the sterile states are only partially thermalized. This can for example happen in models with nonzero lepton asymmetry [26,27]. Therefore, in Sec. IV we perform three different analyses:

(A) All neutrinos are massless. In this case cosmological observables are just sensitive to the total effective number of relativistic (fermionic) degrees of freedom denoted by N_{eff}, where $N_{\mathrm{eff}} = 3.046$ [15] if only (effectively massless) Standard Model neutrinos are present.

(B) Neutrinos are allowed to be massive, with a common total mass $\sum m_\nu$ and a number effectively equal to N'_{eff}. This corresponds to

$$\sum m_\nu = N'_{\mathrm{eff}} \times m_M. \tag{8}$$

(C) The three Standard Model neutrinos are (effectively) massless, while extra sterile neutrinos are present in (effective) number equal to N_S and total (effective) mass equal to m_S. This corresponds to

$$\sum m_{\nu S} = N_S \times m_S \tag{9}$$

and to a total effective number of neutrinos $N_{\mathrm{eff}} = 3.046 + N_S$. This case differs from case (B) since here the presence of three massless neutrinos fully contributes to radiation energy, while in case (B) all neutrinos are effectively massive and there may be a different impact on matter-radiation equality, CMB anisotropies, and cosmic structure formation. Clearly in this case N_S measures only the extra number of degree of freedom responsible for dark radiation, while in case (B) N'_{eff} is the total number of (potentially) massive neutrinos.

We have considered the possibility that sterile neutrinos are only partially thermalized. In our analysis we express this in terms of the following parameter:

$$N_i = \frac{n_i}{n_i^{\mathrm{th}}}, \tag{10}$$

where n_i denotes the actual number density of a sterile neutrino of mass m_i while n_i^{th} denotes the number density of a standard neutrino (fully thermalized, with a Fermi-Dirac phase-space distribution) with the same mass m_i. The multiplicity parameter N_i therefore defines the fractional contribution of the (nonstandardly thermalized) sterile neutrino to the dark matter energy density, and is a number defined in the interval [0, 1]. In our assumptions, N_i is considered to be independent from the mass m_i, and therefore N_i and m_i can be treated as independent parameters in the analysis. While this may not be the most general case, it is generic enough to study the possibility to allow, in the cosmological data, for extra sterile neutrinos endowed with the properties dictated by the SBL studies. Examples of values of $N_i < 1$ may be related to partial thermalization (possibly related to the presence of a lepton asymmetry, since the mixing angles obtained from the SBL analysis are large enough to ensure thermalization of the sterile neutrinos if the asymmetry is absent) or nonstandard phase-space distributions for sterile neutrinos. The limit $N_i = 1$ refers to a fully thermalized Fermi-Dirac sterile neutrino.

In out joint (cosmological + SBL) analysis (discussed in Sec. V) we assume the three active neutrinos as massless and the $\sum m_\nu$ in Eq. (7) is therefore given by $\sum m_\nu = \sum_i N_i m_i$, where the index i runs over the number of sterile neutrinos considered in our analysis,

$$\sum m_\nu = N_4 \times m_4 \quad (3+1), \tag{11}$$

$$\sum m_\nu = N_4 \times m_4 + N_5 \times m_5 \quad (3+2). \tag{12}$$

We have considered a top-hat prior in the range [0, 1] for the multiplicity parameters, while the sterile neutrino masses have been subjected to a prior given by the χ^2 results of the SBL analysis.

Finally, in order to grasp a connection between the joint (cosmological + SBL) analysis and the more typical cosmological investigations (where the relevant parameters are just the sum of the neutrino masses and an effective number of additional light states, as discussed above), we have reanalyzed the (3 + 2) case by using the SBL prior on m_4 and m_5 projected over the sum of the two masses $m_4 + m_5$. This case corresponds again to a situation where

$$\sum m_\nu = N_4 \times m_4 + N_5 \times m_5 \quad (3+2), \tag{13}$$

where we look at the results in terms of $(N_4 + N_5)$ and $m_4 + m_5$. This case is discussed in Sec. V and differs from the case studied in connection with case (C) because information coming from the SBL studies is included in the analysis.

IV. COSMOLOGICAL RESULTS

The cosmological analyses performed on the full CMB data set (WMAP9, SPT, and ACT combined) is shown in Table II. The results for case (B) are also illustrated in Fig. 2, where the marginalized 68% and 95% contours for $N'_{\rm eff}$ and $\sum m_\nu$ are reported. The analysis for the combination of WMAP9 + SPT + ACT data sets refers to the leftmost (red) contours; the further inclusion of BAO + Hubble Space Telescope (HST) moves the contours to the right (blue contours), referring to larger $N'_{\rm eff}$, accompanied by smaller values of $\sum m_\nu$). Figure 3 shows the one-dimensional marginalized posteriors for $N'_{\rm eff}$ and $\sum m_\nu$.

The results shown in Table II and Figs. 2 and 3 point toward the conclusion that the full set of present CMB data do not show any indication for a nonstandard value of the effective number of relativistic degrees of freedom. Nevertheless this result is mostly driven by the new ACT likelihood and a strong tension actually emerges between the new SPT and the new ACT data. This tension results in a bias that has a strong impact on the cosmological results, especially on the neutrino sector. Removing the ACT data and using only WMAP9 and SPT, in the massless neutrino case [case (A)] we recover a 1.5σ evidence for an extra dark radiation component,

$$N_{\rm eff} = 3.87 \pm 0.55 (1\sigma) \quad \text{case (A)} \qquad \text{WMAP + SPT.}$$

TABLE II. Values of the cosmological parameters and their 68% confidence level intervals for the the three cosmological analysis described in Sec. III: case (A) refers to $N_{\rm eff}$ massless neutrinos; case (B) refers to $N'_{\rm eff}$ massive neutrinos with total mass $\sum m_\nu$; case (C) refers to three massless (active) neutrinos plus N_S additional (sterile) neutrinos, with total mass m_S. Upper bounds are quoted at 95% C.L.

Parameters	Case (A) WMAP9 +SPT + ACT	Case (B) WMAP9 +SPT + ACT	Case (C) WMAP9 +SPT + ACT
$\Omega_b h^2$	0.02259 ± 0.00045	0.02224 ± 0.00053	0.02281 ± 0.00035
$\Omega_{\rm dm} h^2$	0.115 ± 0.008	0.120 ± 0.009	0.126 ± 0.009
θ_s	1.0418 ± 0.0013	1.0417 ± 0.0013	1.0416 ± 0.0011
τ	0.086 ± 0.014	0.086 ± 0.013	0.088 ± 0.013
n_s	0.972 ± 0.017	0.959 ± 0.020	0.966 ± 0.010
$\log(10^{10} A_s)$	3.178 ± 0.041	3.213 ± 0.049	3.212 ± 0.039
$N_{\rm eff}$ (A)	3.17 ± 0.47	...	...
$N'_{\rm eff}$ (B)	...	2.97 ± 0.48	...
$\sum m_\nu$ [eV] (B)	...	<1.17	...
N_S (C)	...	...	<0.89
$\Sigma m_{\nu S}$ [eV] (C)	...	...	<2.39
H_0 [km/s/Mpc]	71.7 ± 3.4	64.9 ± 5.5	68.9 ± 2.0
σ_8	0.822 ± 0.029	0.714 ± 0.073	0.699 ± 0.071
$\Omega_{\rm m}$	0.269 ± 0.020	0.345 ± 0.063	0.315 ± 0.034
$a_{t\rm SZ}$	4.4 ± 0.9	4.4 ± 0.9	4.5 ± 0.9
$a_{k\rm SZ}$	<3.2	<3.4	<3.7
a_c	6.0 ± 0.5	6.0 ± 0.5	6.2 ± 0.5
$a_{p\rm SPT}$	18.5 ± 1.6	18.6 ± 1.6	18.4 ± 1.6
$a_{p\rm ACT}$	7.0 ± 0.3	6.9 ± 0.3	6.9 ± 0.3
$\chi^2_{\rm min}$	8962.2	8962.9	8961.3

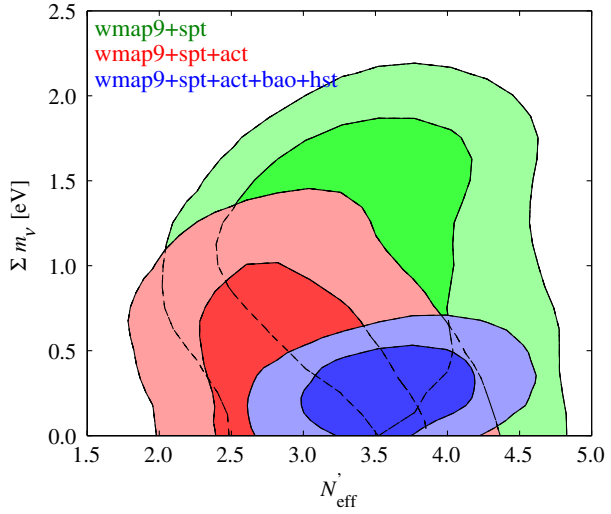

FIG. 2 (color online). Case (B): $N'_{\rm eff}$ massive neutrinos with total mass $\sum m_\nu$. Two-dimensional marginalized 68% and 95% confidence level regions in the plane $\sum m_\nu$ versus $N'_{\rm eff}$. Leftmost (red) contours refer to CMB-only data (WMAP9 + SPT + ACT), while rightmost (blue) contours also include BAO and HST. The larger (green) area denotes the results for WMAP9 + SPT data sets.

This result is fully consistent with those of the WMAP9 [19] and SPT [20] analyses. In the case of massive neutrinos [case (B)] Fig. 2 shows that, when all CMB data are considered (red contours), an anticorrelation emerges between $N'_{\rm eff}$ and the total mass $\sum m_\nu$: a higher value of the sum of the masses seems to be consistent with a lower value of the number of neutrinos that share the same mass. This inconsistency can be traced to the tension between the high-multipole data sets (ACT and SPT). Indeed, excluding the ACT data, we get the green contour of Fig. 2: the higher-mass values allowed by SPT correspond to higher numbers of neutrino species, and there is not a strong correlation between these two quantities. Furthermore the above tension between ACT and SPT is also less pronounced if we take into account BAO and HST data. In this case (blue contours) we recover the expected positive correlation between $\sum m_\nu$ and $N'_{\rm eff}$, because the HST measurements fix the expansion rate and, as a consequence, the dimension of the sound horizon at recombination and the damping scale. So an enhancement in the sum of the masses is needed in order to get a higher value of the number of neutrino species. Moreover, considering WMAP9 + SPT + ACT + BAO + HST, we get a slight preference for a nonstandard value of the effective number of relativistic degrees of freedom (see Fig. 3),

$$N'_{\rm eff} = 3.60 \pm 0.35(1\sigma) \quad \text{case (B)}$$
$$\text{WMAP + SPT + ACT + BAO + HST.}$$

Concerning the mass, the constraint on $\sum m_\nu$ is significantly tightened by adding the low-redshift observations (BAO and HST) data and it turns out to be

$$\sum m_\nu < 0.59 \text{ eV}(95\% \text{ C.L.}) \quad \text{case (B)}$$
$$\text{WMAP + SPT + ACT + BAO + HST,}$$

with a best fit value of $\sum m_\nu = 0.23$ eV, as we can see in Fig. 3.

Excluding ACT data and using only WMAP9 + SPT, in the case of massive neutrinos [case(B)], we obtain

$$N'_{\rm eff} = 3.44 \pm 0.56(1\sigma) \quad \text{case (B)} \qquad \text{WMAP + SPT,}$$

with a total mass

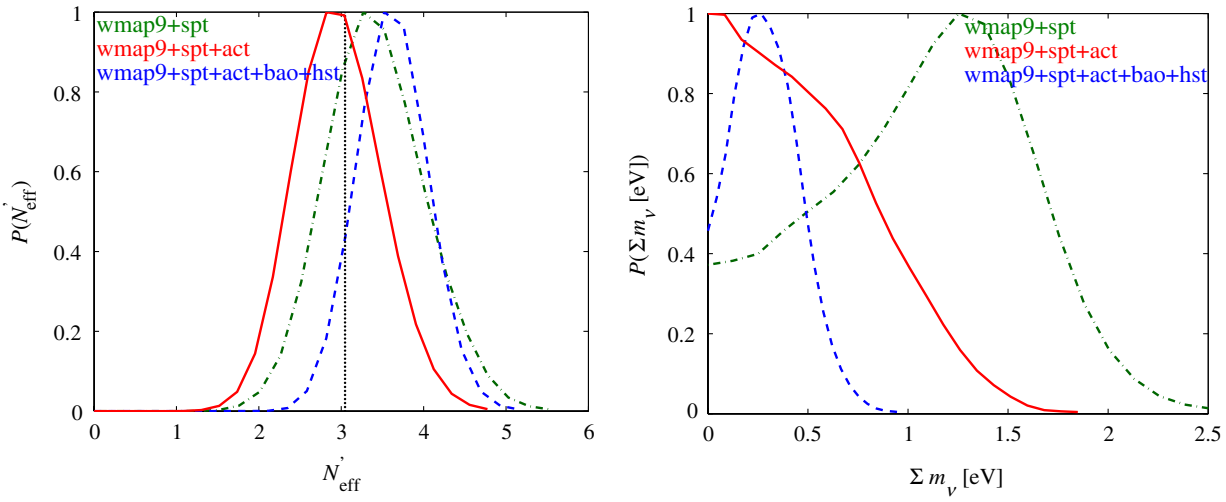

FIG. 3 (color online). Case (B): $N'_{\rm eff}$ massive neutrinos with total mass $\sum m_\nu$. One-dimensional marginalized posteriors for $N'_{\rm eff}$ (left panel) and $\sum m_\nu$ (right panel). Solid (red) lines refer to CMB-only data (WMAP9 + SPT + ACT), while dashed (blue) lines also include BAO and HST. The dot-dashed (green) curve denotes the results for WMAP9 + SPT data sets.

$$\sum m_\nu < 1.85 \text{ eV}(95\% \text{ C.L.}) \quad \text{case (B)}$$

WMAP + SPT.

In Fig. 3 the dot-dashed (green) line shows the one-dimensional marginalized posteriors for $\sum m_\nu$ and $N'_{\rm eff}$ in this case with only WMAP9 + SPT. The best-fit value for the sum of the masses is shifted beyond 1 eV and the range of possible mass values is much less constrained than in the above cases when ACT data are included.

V. JOINT ANALYSIS

Since the new SPT [20] and ACT [21] data seem to point towards opposite directions concerning the effective number of relativistic degrees of freedom, here we adopt the conservative approach to not combine the two data sets in the joint analysis with SBL experiments.

Moreover, we decided to consider only the SPT data set for the following reasons. First of all, the ACT data set, when only the temperature angular power spectrum data is considered, provides an indication for gravitational lensing larger by ~70% than that expected in the standard ΛCDM model (with massless neutrinos) at more than 95% C.L. (see Ref. [21] but also Ref. [58]). Since massive neutrinos decrease the gravitational lensing signal, the lensing anomaly biases the ACT results on neutrino masses towards more stringent constraints (see Fig. 3, right panel of Ref. [58]). The origin of this anomalous signal is unclear and could possibly be due to a systematic error in the data. The SPT data set, on the other hand, exhibits no anomaly in the lensing signal.

Secondly, ACT is composed of two maps in two different regions of the sky, defined respectively as the ACT-E and the ACT-S data sets. The ACT-S map overlaps with the region sampled by SPT and the two should not be combined because of their covariance. The ACT-E data set (which constitutes approximately 50% of the entire data set) provides constraints that are even in larger tension with SPT (see Ref. [21]).

In what follows we report the results for the joint (cosmological + SBL) analysis, obtained with different combinations of cosmological data sets. The SBL posterior probabilities on the neutrino parameters are used as priors in the MCMC sampling of those parameters relevant to cosmology, i.e. the sterile neutrino masses. In the (3 + 1) scheme we have a prior on the single extra neutrino mass m_4; in the (3 + 2) scheme we have priors for the two extra neutrino masses m_4 and m_5; finally, in the (3 + 2) scheme we also consider the only relevant parameter for cosmology, which is the sum of the neutrino masses $m_4 + m_5$ and for that we use a prior obtained from the SBL analysis by projecting the SBL priors for the single masses to the sum of the two.

A. (3 + 1) joint analysis

The results of the joint (cosmological + SBL) analysis for the (3 + 1) scheme are reported in Table III and in Figs. 4 and 5. The analysis refers to the case of Eq. (11). In this analysis, in addition to the CMB data sets (WMAP9 [19] and SPT [20]) we also consider information on the matter power spectrum coming from large scale observables: we include data from the Sloan Digital Sky Survey Data Release 7 (SDSS) [53].

When only cosmological data is used, bounds on N_4 and m_4 are broad: the allowance for an extra neutrino which cosmologically acts only as a fraction of a fully thermalized one is compatible with cosmological data for a neutrino mass as large as 2.09 eV. The bound on the multiplicity parameter N_4 is as large as 0.96. These results stand when SDSS data are also included; CMB-only data, instead, have a preference for lower values of N_4 and m_4, with best-fit values different from zero at about the 3σ level. The central value for N_4 is 0.65 and deviates from

TABLE III. (3 + 1) analysis. Values of the cosmological parameters and their 68% confidence-level intervals in the case of one additional massive sterile neutrino, with mass m_4 and with multiplicity N_4. The (3 + 1) SBL χ^2 is applied where specified. Upper bounds are quoted at 95% C.L.

Parameters	WMAP9 + SPT	WMAP9 + SPT + SBL	WMAP9 + SPT + SDSS	WMAP9 + SPT + SDSS + SBL
$\Omega_b h^2$	0.02256 ± 0.00037	0.02249 ± 0.00035	0.02233 ± 0.00034	0.02230 ± 0.00034
$\Omega_{\rm dm} h^2$	0.131 ± 0.008	0.131 ± 0.007	0.127 ± 0.007	0.128 ± 0.007
θ_s	1.0412 ± 0.0011	1.0411 ± 0.0011	1.0411 ± 0.0011	1.0412 ± 0.0010
τ	0.083 ± 0.013	0.083 ± 0.013	0.081 ± 0.012	0.080 ± 0.012
n_s	0.959 ± 0.011	0.962 ± 0.009	0.963 ± 0.011	0.958 ± 0.009
$\log(10^{10} A_s)$	3.222 ± 0.041	3.218 ± 0.036	3.212 ± 0.036	3.226 ± 0.034
N_4	0.65 ± 0.22	0.69 ± 0.21	<0.96	<0.83
m_4 [eV]	1.72 ± 0.65	1.27 ± 0.12	<2.09	1.23 ± 0.13
H_0 [km/s/Mpc]	68.6 ± 2.1	68.9 ± 1.7	69.3 ± 1.9	68.1 ± 1.4
σ_8	0.668 ± 0.061	0.692 ± 0.036	0.766 ± 0.036	0.744 ± 0.034
$\Omega_{\rm m}$	0.327 ± 0.035	0.325 ± 0.030	0.311 ± 0.025	0.324 ± 0.027
$\chi^2_{\rm min}$	8274.1	8274.3	8326.4	8327.5

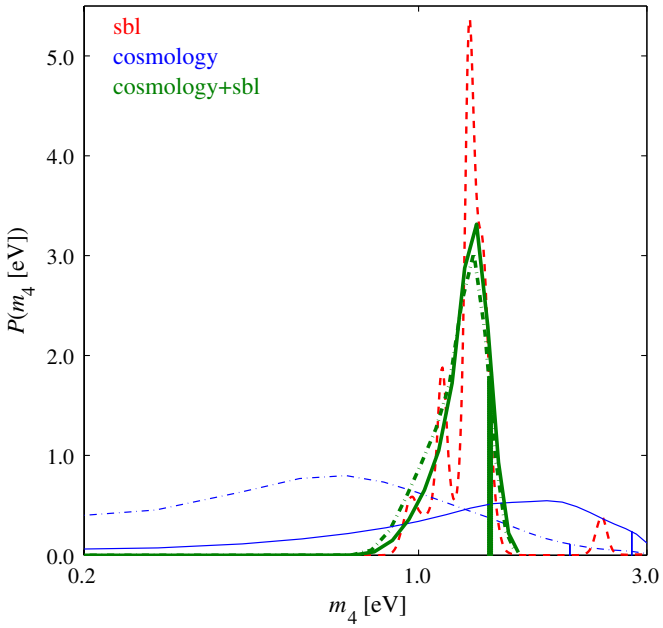

FIG. 4 (color online). (3 + 1) analysis. One-dimensional marginalized posterior for m_4. The thick (green) and thin (blue) lines refer to the case of Table III with and without the SBL prior, respectively. Solid lines stand for the analysis on CMB-only (WMAP9 + SPT) data; dot-dashed lines refer to the inclusion of information from the matter power spectrum. The (red) dashed line shows the 3 + 1 SBL posterior. 95% C.L. upper bounds on the mass for the different cases are reported as vertical lines.

zero at 2.9σ; the preferred value for m_4 is 1.72 eV, and differs from zero at the 2.7σ level.

When the SBL posterior probability on m_4 in used as a prior in the cosmological analysis, the situations moves toward a clear preference for a neutrino mass above 1 eV and slightly lower values for the multiplicity parameter. The result on the mass is expected, since SBL data have a clear preference for a nonzero neutrino mass, and this reflects on the posterior probabilities of the joint analysis. The combination of CMB-only data with SBL results does not appreciably change the multiplicity parameter (preferred value of 0.69, different from zero at the 3σ level) while it slightly reduces the best-fit value for the mass: 1.27 eV, with an error of 0.12. The inclusion of SDSS data enlarges the allowed interval for the multiplicity parameter, while the preferred value for the masses is further decreased to 1.23 eV, with an error of 0.13, incompatible with zero at high significance.

Figure 4 shows the one-dimensional marginalized posteriors of the joint analyses for m_4 in all the cases reported in Table III, together with the SBL posterior of the (3 + 1) analysis. Concerning the SBL posterior we can appreciate that the zero-mass region is highly excluded and the maximum probability is characterized by three peaks between 1 and 2 eV, plus a small peak close to 3 eV. In the combined analysis (which includes the SBL posterior as a prior), the joint posterior closely follows the SBL posterior, with basically the same best fit located at $m_4 = 1.27$ eV. The only relevant difference of the joint posterior with respect to the SBL posterior is the suppression in the joint posterior of the SBL high-mass peak close to 3 eV, which is in fact highly disfavored by cosmological data, especially when the matter power spectrum is included in the analysis. We notice also that the inclusion of SBL information alleviates the tension between CMB and the matter power spectrum: in fact, CMB-only data exhibit a best-fit value close to 2 eV

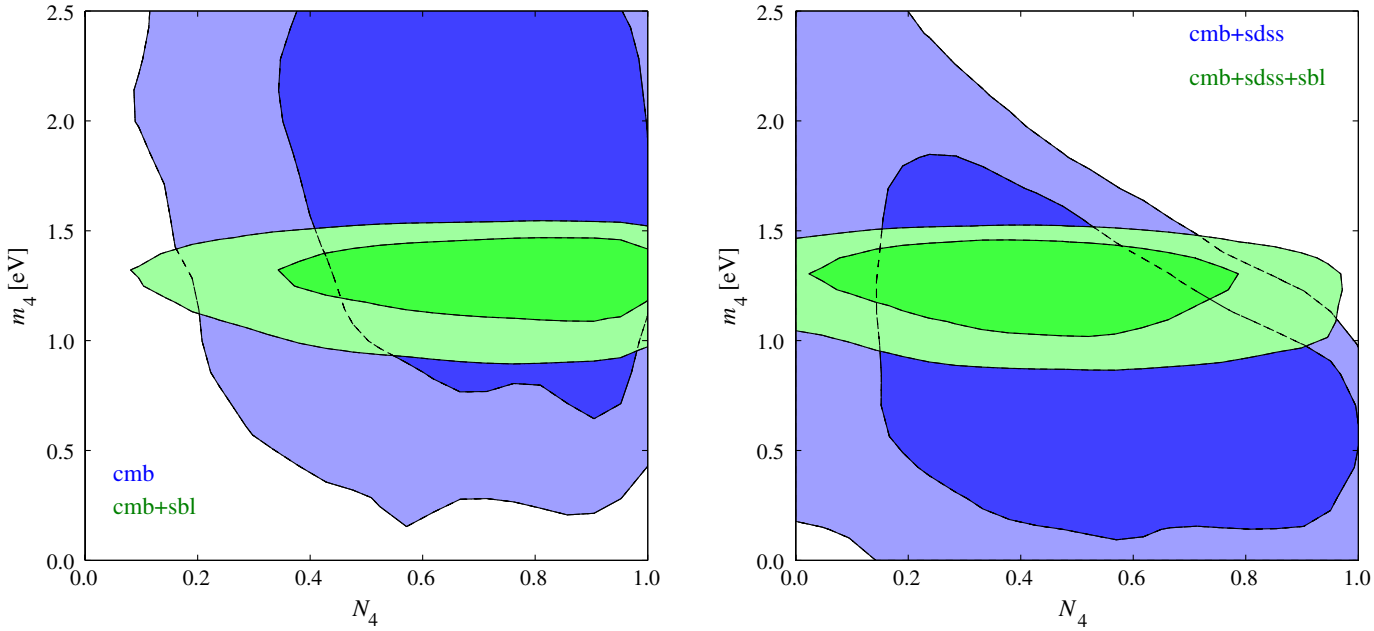

FIG. 5 (color online). (3 + 1) analysis. Two-dimensional marginalized 68% and 95% confidence-level regions in the plane $N_4 - m_4$ for the different combinations of data sets reported in Table III.

and a detection of the single mass eigenstate $m_4 = (1.72 \pm 0.65)$ eV, while the inclusion of SDSS data shifts the results towards lower values of m_4 and is consistent with a zero value of the mass eigenstate.

As discussed above, the value of N_4 is almost unconstrained when SDSS data are included, while in the case of CMB-only data there is evidence for an extra massive sterile neutrino. This is also manifest in Fig. 5, where the two-dimensional marginalized 68% and 95% C.L. regions in the plane (N_4, m_4) are plotted for the different combinations of data sets reported in Table III. We can clearly see the effect of the SBL data: the constraints on the mass are strongly tightened but there is almost no effect on N_4. Concerning the degeneracy between the number of sterile states and their mass, a negative correlation emerges when the matter power spectrum is taken into account and the result is a divergence of m_4 as N_ν^4 is approaching zero.

B. Bidimensional (3 + 2) joint analysis

The results of the joint analysis for the (3 + 2) scheme are reported in Table IV and in Figs. 6 and 7. The analysis refers to the case of Eq. (12).

Concerning the masses, the value of the heaviest mass eigenstate (m_5) is always significantly deviating from zero: when CMB-only data are considered the effect is at the 3.5σ when the SBL are not included, and grows to a 4σ effect when SBL priors are considered. In both cases, the neutrino mass is around 2 eV. When large-scale-structure data are included, the preferred value for the mass decreases around 1.5 eV, with a significance of $2.1(3.2)\sigma$ without (with) the inclusion of SBL data. SBL results, which have a clear preference for massive neutrinos close to 1.6 eV, reinforce the cosmological results and therefore induce a clear increase in the confidence for the mass determination. This fact occurs also for the lighter mass eigenstate (m_5). While cosmological data do not require the lightest neutrino to be massive (bounds are at 2.11 eV for CMB-only data and 1.34 eV when SDSS is included), SBL priors also induce a clear preference for a nonzero lightest mass eigenstate around 1 eV (an effect close to the 4σ level).

The multiplicity parameter of each mass eigenstate is basically unconstrained for all the different combinations of data sets. Full and standard thermalization ($N_i = 1$, $i = 3, 4$) is not allowed, but fractional occupations as large as 0.92 are possible. A notable exception occurs for the heaviest eigenstate (m_5) when SDSS data are included; in this case, the multiplicity parameter needs to be smaller, not exceeding 0.78 for the full combination of cosmological data and further decreasing to 0.62 when the SBL information is included. From the last column of Table IV we can conclude that cosmological and SBL data are consistent with the existence of two extra sterile neutrinos, provided that they are not fully thermalized.

The same results can be appreciated in more detail by directly looking at the behavior of posterior probabilities. Figure 6 shows the one-dimensional marginalized posterior for m_4 (left panel) and m_5 (right panel) in all the cases reported in Table IV, together with the SBL posteriors of the (3 + 2) scheme, marginalized over the parameters not shown in the figure. The SBL posteriors are characterized by the clear exclusion of zero values for both m_4 and m_5. The cosmological posteriors of m_4 prefer a zero mass value, even more so when the matter power spectrum information is included in the analysis. When the SBL χ^2 information is applied, the null values for the neutrino masses become clearly disfavored. The matter-power-spectrum effect results in a shift of the preferred mass range towards lower values.

TABLE IV. (3 + 2) analysis. Values of the cosmological parameters and their 68% confidence-level intervals in the case of two additional massive sterile neutrinos, with masses m_4 and m_5 multiplicities N_4 and N_5. The bidimensional (3 + 2) SBL χ^2 is applied where specified. Upper bounds are quoted at 95% C.L.

Parameters	WMAP9 + SPT	WMAP9 + SPT + SBL	WMAP9 + SPT + SDSS	WMAP9 + SPT + SDSS + SBL
$\Omega_b h^2$	0.02270 ± 0.00038	0.02267 ± 0.00037	0.02242 ± 0.00036	0.02235 ± 0.00035
$\Omega_{\rm dm} h^2$	0.139 ± 0.010	0.139 ± 0.009	0.133 ± 0.008	0.131 ± 0.008
θ_s	1.0408 ± 0.0011	1.0409 ± 0.0011	1.0406 ± 0.0011	1.0409 ± 0.0011
τ	0.083 ± 0.013	0.083 ± 0.013	0.082 ± 0.013	0.080 ± 0.012
n_s	0.961 ± 0.012	0.960 ± 0.010	0.967 ± 0.012	0.960 ± 0.010
$\log(10^{10} A_s)$	3.228 ± 0.041	3.232 ± 0.038	3.213 ± 0.037	3.225 ± 0.034
N_4	<0.92	<0.92	<0.92	<0.85
m_4 [eV]	<2.11	1.20 ± 0.30	<1.34	0.95 ± 0.30
N_5	<0.93	<0.91	<0.78	<0.62
m_5 [eV]	2.07 ± 0.58	1.96 ± 0.48	1.45 ± 0.67	1.59 ± 0.49
H_0 [km/s/Mpc]	68.5 ± 2.3	67.9 ± 1.9	69.6 ± 2.1	68.2 ± 1.5
σ_8	0.642 ± 0.060	0.648 ± 0.037	0.752 ± 0.036	0.734 ± 0.032
$\Omega_{\rm m}$	0.346 ± 0.038	0.352 ± 0.037	0.321 ± 0.027	0.331 ± 0.026
$\chi^2_{\rm min}$	8274.1	8274.8	8326.4	8327.8

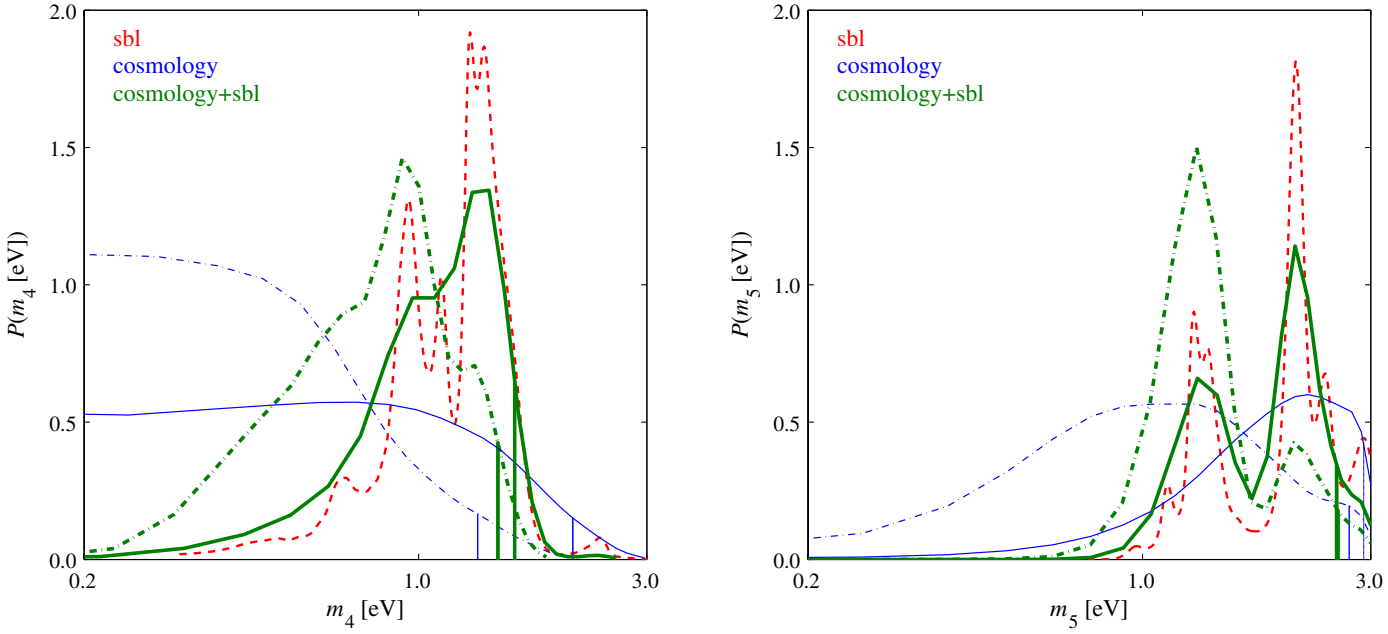

FIG. 6 (color online). (3 + 2) analysis. One-dimensional marginalized posterior probabilities for m_4 (left panel) and m_5 (right panel). The thick (green) and thin (blue) lines refer to the case of Table IV with and without SBL prior, respectively. Solid lines stand for the analysis on CMB-only (WMAP9 + SPT) data; dot-dashed lines refer to the inclusion of information coming from the matter power spectrum. The (red) dashed line shows the bidimensional 3 + 2 SBL posterior marginalized over m_4 or m_5. 95% C.L. upper bounds on the masses are reported as vertical lines.

Figure 7 shows the two-dimensional marginalized 68% and 95% confidence regions in the plane $m_4 - m_5$ for the different combinations of data sets reported in Table IV, plus the two-dimensional marginalized 95% SBL posterior of the 3 + 2 model. Even when the matter power spectrum is included in the cosmological analysis, the blue contours referring to cosmological data only show a good agreement with the red 2σ confidence region obtained by the SBL analysis.

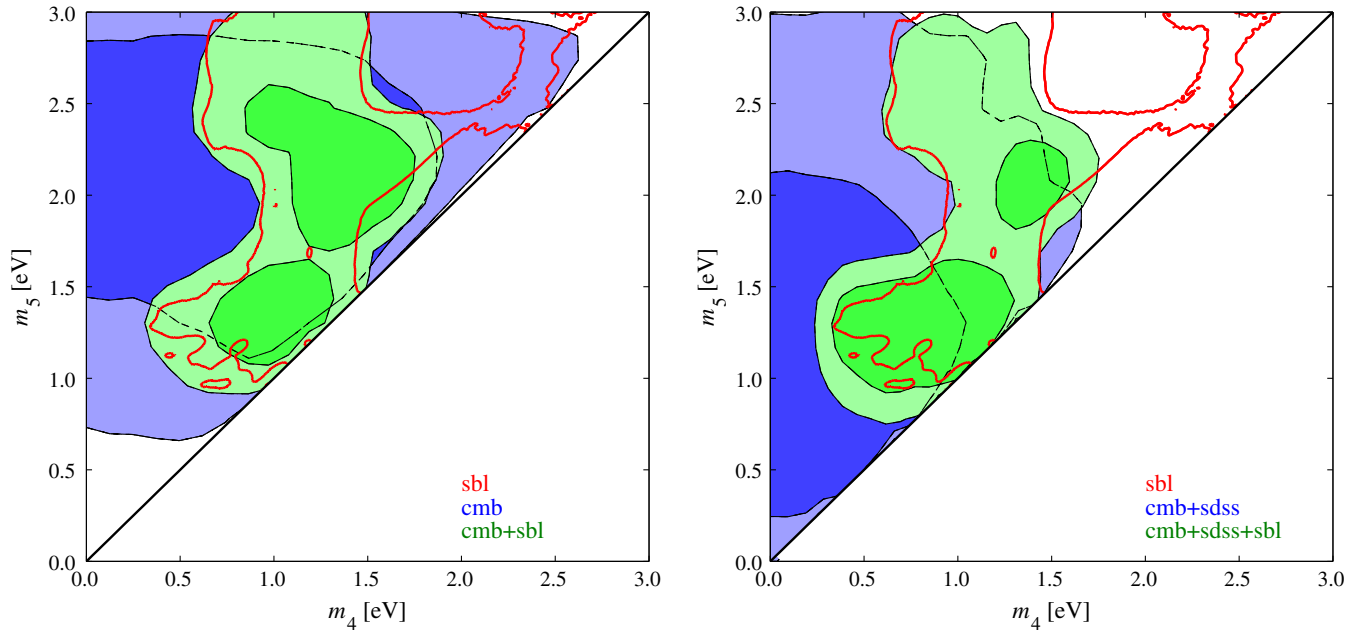

FIG. 7 (color online). (3 + 2) analysis. Two-dimensional marginalized 68% and 95% confidence-level regions in the plane ($m_4 - m_5$) for the different combinations of data sets reported in Table IV. The two-dimensional marginalized 95% SBL posterior probability of the 3 + 2 model is also overplotted (red solid line).

TABLE V. Reduced (3 + 2) analysis. Values of the cosmological parameters and their 68% confidence-level intervals, for the data analyzed in terms of of the sum of the sterile neutrino mass eigenstates ($m_4 + m_5$) and of their total effective multiplicity $N_4 + N_5$. The one-dimensional (3 + 2) SBL χ^2 is applied where specified. Upper bounds are quoted at 95% C.L.

Parameters	WMAP9 + SPT	WMAP9 + SPT + SBL	WMAP9 + SPT + SDSS	WMAP9 + SPT + SDSS + SBL
$\Omega_b h^2$	0.02270 ± 0.00038	0.02270 ± 0.00039	0.02242 ± 0.00036	0.02241 ± 0.00035
$\Omega_{\rm dm} h^2$	0.139 ± 0.010	0.139 ± 0.009	0.133 ± 0.008	0.132 ± 0.008
θ_s	1.0408 ± 0.0011	1.0407 ± 0.0011	1.0406 ± 0.0011	1.0407 ± 0.0011
τ	0.083 ± 0.013	0.084 ± 0.013	0.082 ± 0.013	0.081 ± 0.012
n_s	0.961 ± 0.012	0.963 ± 0.011	0.966 ± 0.012	0.964 ± 0.010
$\log(10^{10} A_s)$	3.228 ± 0.041	3.225 ± 0.040	3.213 ± 0.037	3.217 ± 0.035
$N_4 + N_5$	0.97 ± 0.31	1.00 ± 0.31	0.75 ± 0.32	0.69 ± 0.29
$(m_4 + m_5)$ [eV]	3.04 ± 0.97	2.80 ± 0.71	1.98 ± 0.89	2.33 ± 0.61
H_0 [km/s/Mpc]	68.5 ± 2.3	68.7 ± 2.2	69.6 ± 2.1	69.1 ± 1.8
σ_8	0.642 ± 0.060	0.647 ± 0.054	0.752 ± 0.036	0.744 ± 0.033
$\Omega_{\rm m}$	0.346 ± 0.038	0.344 ± 0.037	0.321 ± 0.027	0.325 ± 0.026
$\chi^2_{\rm min}$	8274.1	8275.1	8326.4	8327.6

C. Reduced (3 + 2) joint analysis

Finally, in Table V and in Figs. 8 and 9 we show the results of the joint (cosmological + SBL) analysis in the (3 + 2) scheme, where we have postprocessed the chains of the MCMC to get constraints only on the sum of the mass eigenstates and on the total number of extra species, by applying an SBL prior on $(m_4 + m_5)$ obtained by realizing a one-dimensional SBL posterior on the sum of the two masses.

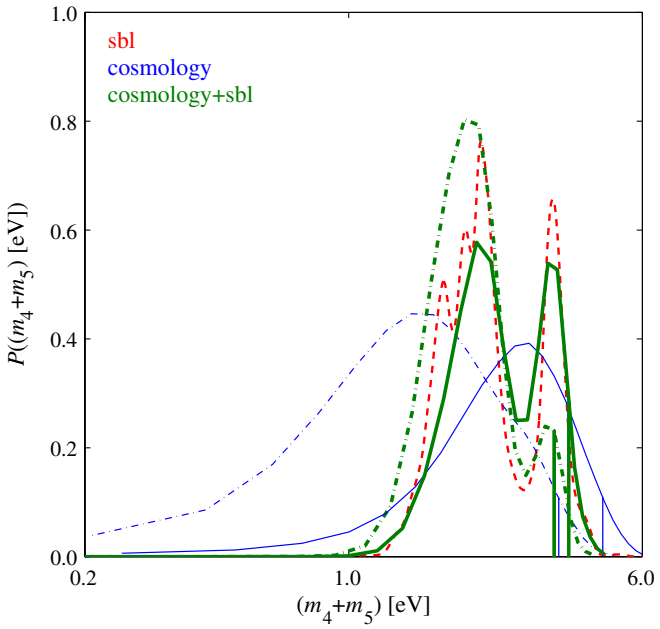

FIG. 8 (color online). Reduced (3 + 2) analysis. One-dimensional marginalized posterior probabilities for $(m_4 + m_5)$. The thick (green) and thin (blue) lines refer to the case of Table V with and without SBL prior, respectively. Solid lines stand for the analysis of CMB-only (WMAP9 + SPT) data; dot-dashed refer to the inclusion of information from the matter power spectrum. The (red) dashed line shows the one-dimensional 3 + 2 SBL posterior on $(m_4 + m_5)$. 95% C.L. upper bounds are also reported (vertical lines).

Interestingly in this case the sum of the neutrino masses always shows a clear preference for a nonzero value, even when only cosmological data are considered: the confidence level for CMB-only data is 3.1σ, and degrades to 2.2σ when SDSS data are included. The inclusion of the SBL information sizably strengthen the result, driving the confidence of nonzero masses close to a 4σ level.

Figure 8 shows these behaviors by reporting the one-dimensional marginalized posterior for $m_4 + m_5$ in all the cases reported in Table V, together with the posteriors obtained by analyzing the SBL data within the framework of the (3 + 2) model and marginalizing over $m_4 + m_5$. The situation is analogous to the one we found in Sec. V B. The cosmological posteriors alone show a preference for a nonzero value for the sum of the masses. As usual, when SDSS data are considered, the posterior is shifted towards lower values for the sum of the masses, but the preference remains for masses around 1 eV. Concerning the SBL posterior, the maximum probability on the sum of the masses is around 2 eV as expected, with a tail at higher masses. This higher-mass tail is suppressed in the joint posterior, when the cosmological analysis also considers the matter-power-spectrum information. Instead, a higher-mass tail can be seen in the joint posterior when the combined analysis takes into account CMB-only data as cosmological data sets.

Figure 9 shows the two-dimensional marginalized 68% and 95% confidence-level regions in the plane $(N_4 + N_5)$ versus $(m_4 + m_5)$, for the different combinations of data sets reported in Table V. Once again, we can clearly see the effect of the SBL data: the constraints on the sum of the masses are tightened but there is almost no effect on the number of extra massive sterile neutrino species. Furthermore, in Fig. 9 we recognize the same degeneracy between the sum of the mass eigenstates and their multiplicity that was seen in Fig. 5. As we have already discussed, this degeneracy appears when matter-power-spectrum information is taken into account. Interestingly, here this degeneracy also remains when the SBL posterior is applied.

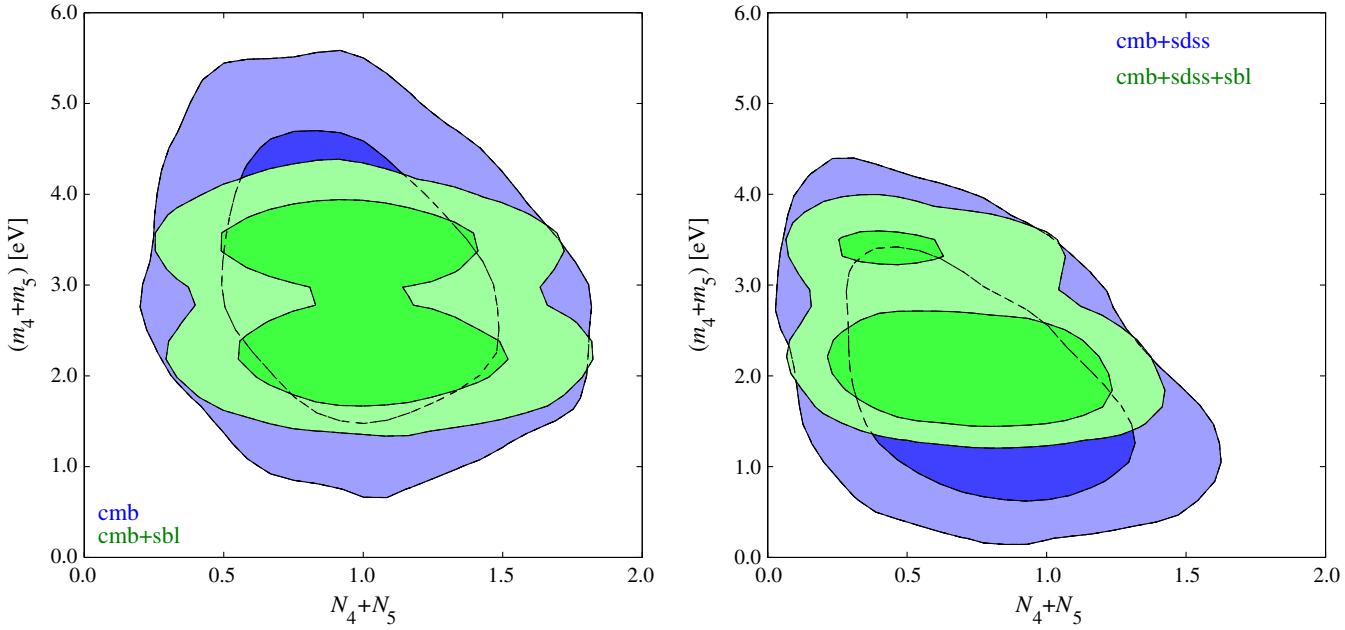

FIG. 9 (color online). Reduced (3 + 2) analysis. Two-dimensional marginalized 68% and 95% confidence-level regions in the plane $(N_4 + N_5)$ versus $(m_4 + m_5)$ for the different combinations of data sets reported in Table V.

VI. CONCLUSIONS

The case for extra dark radiation in cosmology has recently become very complex and somewhat controversial: the new WMAP9 and SPT data are still pointing toward an extra component while the new ACT results became compatible with the standard cosmological value $N_{\rm eff} = 3.046$. On the other hand short-baseline neutrino oscillation experiments keep confirming the LSND anomaly and the presence of one or two sterile neutrinos.

In this framework, our analysis provides an update of the cosmological results in the sterile neutrino context, taking into account all the present CMB data (WMAP9, SPT, ACT) and investigating all the possible parametrizations (massless; massive; three active massless plus a varying number of massive sterile states).

We find that even in the context of such very general models the ACT and SPT data are not compatible, and that the results are strongly affected by this discrepancy. This in turn affects the inferred neutrino mixing and thermalization parameters. The discrepancy is to some extent alleviated when BAO data plus a prior on H_0 from the HST analysis are included; in this case the effective number of (massive) neutrinos is 3.60 ± 0.35 with a total effective mass 0.59 eV.

Given this discrepancy we have not used the ACT data set in the rest of our analysis (because it also leads to spuriously stringent bounds on the neutrino mass), and we considered only WMAP9 and SPT in combination with SDSS-DR7. In order to analyze the cosmological evidences in the context of neutrino-mass models and short-baseline neutrino oscillation data, we have used the results from the SBL as a prior in the analyses of cosmological data. We specifically considered models with one or two extra sterile neutrinos [denoted by (3 + 1) and (3 + 2) schemes]: we first performed a full analysis of the SBL data and then we used the SBL posterior probabilities on the sterile neutrino masses as priors in the MCMC analysis of the cosmological data sets.

We found that the inclusion of the SBL priors induce tight bounds on the sterile neutrino mass eigenstates, and mildly constrain the fractional contribution of the extra neutrinos to the total energy budget. In the (3 + 1) scheme we obtained $m_4 = (1.27 \pm 0.12)$ eV when CMB-only data are considered as cosmological data sets, and $m_4 = (1.23 \pm 0.13)$ eV when SDSS–DR7 data are also included. We also noticed that there is evidence for a nonzero value of the single mass eigenstate (although with a larger uncertainty) even without SBL priors when only CMB data are considered: $m_4 = (1.72 \pm 0.65)$ eV. In the (3 + 1) scheme, the inclusion of SBL information does not significantly constrain the multiplicity parameter, which could be as large as 0.96. Instead, if SDSS data are not included in the analysis, the multiplicity parameter can deviate from zero at about 3σ.

In the (3 + 2) context, the inclusion of SBL information induces relatively tight intervals for the two mass eigenstates: $m_4 = (1.20 \pm 0.30)$ eV and $m_5 = (1.96 \pm 0.48)$ eV for CMB-only data; $m_4 = (0.95 \pm 0.30)$ eV and $m_5 = (1.59 \pm 0.49)$ eV when SDSS-DR7 is also included. In this scheme, the multiplicity parameters are again only slightly bounded from above, except for the heaviest mass eigenstate: when SDSS data are included, N_5 cannot exceed 0.62, meaning that the sterile neutrino is only partially contributing to the energy density of the Universe.

In conclusion, we found that the SBL data exhibit a good agreement with the new updated cosmological bounds on

TABLE VI. (3 + 1) analysis. Values of the cosmological parameters and their 68% confidence-level intervals in the case of one additional massive sterile neutrino, with mass m_4 and with multiplicity N_4. The (3 + 1) SBL χ^2 is applied where specified. Upper bounds are quoted at 95% C.L.

Parameters	Planck + HST	Planck + HST + SBL
$\Omega_b h^2$	0.02287 ± 0.00035	0.02290 ± 0.00037
$\Omega_c h^2$	0.1226 ± 0.0048	0.1180 ± 0.0039
θ_s	1.0408 ± 0.0008	1.0414 ± 0.0008
τ	0.092 ± 0.014	0.091 ± 0.013
n_s	0.986 ± 0.010	0.979 ± 0.009
$\log(10^{10} A_s)$	3.144 ± 0.037	3.157 ± 0.034
N_4	0.62 ± 0.25	0.42 ± 0.25
m_4 [eV]	<1.64	1.21 ± 0.14
A_L	1.29 ± 0.13	1.34 ± 0.13
H_0 [km/s/Mpc]	72.1 ± 2.0	70.0 ± 1.3
σ_8	0.793 ± 0.041	0.741 ± 0.042
Ω_m	0.286 ± 0.019	0.299 ± 0.021

neutrino masses; this occurs both when considering CMB-only data (WMAP + SPT) and when adding information from SDSS. Either one or two extra sterile neutrinos, with a mass at (or even above) the eV scale (as dictated by the SBL results) and not fully contributing to the energy density (as can occur, e.g., in the case of partial thermalization) are therefore fully compatible with current cosmological measurements.

VII. PLANCK RESULTS

A few weeks after the completion of this paper, the Planck Collaboration released its results [33]. Concerning the effective number of relativistic degrees of freedom, Planck data combined with WMAP-9 polarization data and high-l data (both ACT and SPT) found $N_{\rm eff}$ consistent with the standard value within 1σ. This result is deeply affected by the Planck measure of the Hubble constant: if the HST prior on H_0 is considered, Planck results recover a 2σ evidence of dark radiation, with an evidence slightly weaker if BAO data are included. The impact of Planck data on dark radiation results strongly depend on the additional data set considered in the analyses. Furthermore even considering the most stringent results, a mild evidence of an extra component of the radiation content of the Universe is still present in the latest data.

In order to check the consistency of our conclusions with the latest CMB data, we have applied our 3 + 1 model to Planck data, including also WMAP-9 polarization and the HST prior on H_0. In this case we also let the lensing amplitude A_L vary according to the definition given in Ref. [59]. As was clearly shown in Ref. [33], the inclusion of a variation in the lensing amplitude of the temperature spectrum is needed in order to avoid biased results on the neutrino mass. Our choice of including the lensing amplitude is indeed motivated by the higher sensitivity of Planck: now the dominant effect of massive neutrinos is related to the gravitational lensing rather than to the early-Integrated Sachs Wolfe effect. In Table VI the new results are reported and it is clear that they still allow for an interpretation of an extra dark radiation component in terms of partially thermalized sterile neutrinos: N_4 turns out to be almost unconstrained and the 95% upper bound on m_4 is consistent with the mass region allowed by SBL posterior [thin (blue) solid line and red dotted line, respectively, in Fig. 10]. As a consequence the joint analysis [thick (green) solid line in Fig. 10] is still acceptable and the joint posterior perfectly matches the SBL. Figure 11

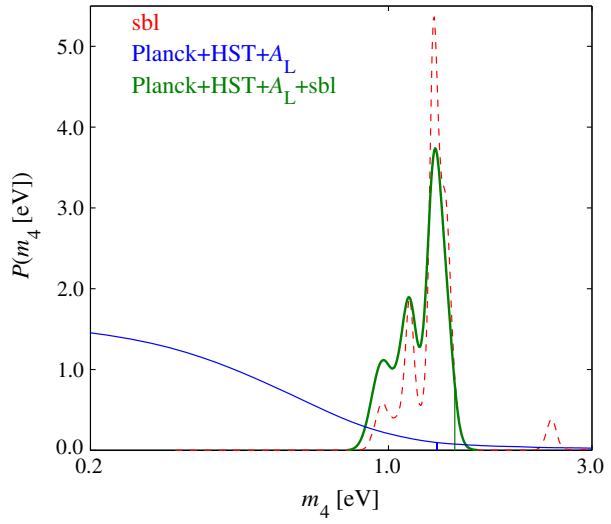

FIG. 10 (color online). (3 + 1) analysis. One-dimensional marginalized posterior for m_4. The thick (green) and thin (blue) lines refer to the case of Table VI with and without the SBL prior, respectively. The (red) dashed line shows the 3 + 1 SBL posterior. 95% C.L. upper bounds on the mass for the different cases are reported as vertical lines.

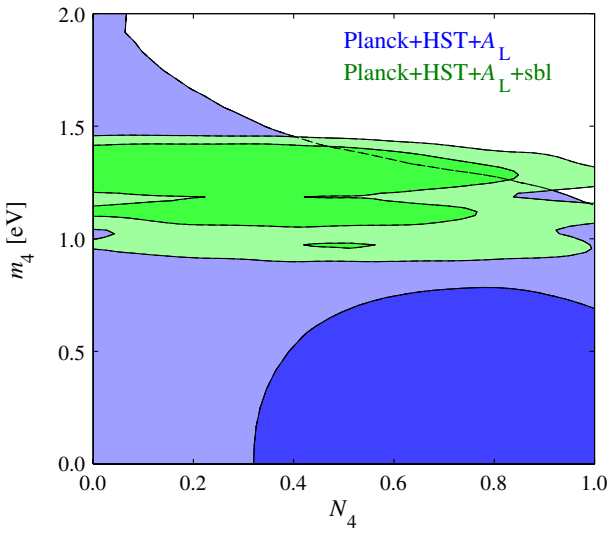

FIG. 11 (color online). (3 + 1) analysis. Two-dimensional marginalized 68% and 95% confidence-level regions in the plane $N_4 - m_4$.

shows that there is no degeneracy among N_4 and m_4 even when only cosmological data are included and the SBL prior is taken out. The reason is that Planck's accuracy makes it possible to resolve the neutrino mass and neutrino number separately. Finally we can appreciate the effect of the SBL prior on the cosmological data. This effect concerns only the sterile mass eigenstate m_4 but it doesn't affect the constraints on the multiplicity N_4. The results presented in this paper are therefore compatible with the new Planck results. We will present a more detailed analysis of the Planck data, in combination with other data sets, in a forthcoming paper [60].

ACKNOWLEDGMENTS

M. A. acknowledges the European ITN project Invisibles (FP7-PEOPLE-2011-ITN, PITN-GA-2011-289442-INVISIBLES). N. F. and C. G. acknowledge INFN research grant FA51. N. F. acknowledges support of the Spanish MICINN Consolider Ingenio 2010 Programme under grant MULTIDARK CSD2009- 00064 (MICINN).

[1] G. L. Fogli, E. Lisi, A. Marrone, D. Montanino, A. Palazzo, and A. M. Rotunno, Phys. Rev. D **86**, 013012 (2012).
[2] J. Kopp, M. Maltoni, and T. Schwetz, Phys. Rev. Lett. **107**, 091801 (2011).
[3] C. Giunti and M. Laveder, Phys. Rev. D **84**, 073008 (2011).
[4] C. Giunti and M. Laveder, Phys. Rev. D **84**, 093006 (2011).
[5] C. Giunti and M. Laveder, Phys. Lett. B **706**, 200 (2011).
[6] G. Karagiorgi, M. H. Shaevitz, and J. M. Conrad, arXiv:1202.1024.
[7] A. Donini, P. Hernandez, J. Lopez-Pavon, M. Maltoni, and T. Schwetz, J. High Energy Phys. 07 (2012) 161.
[8] Z. Hou, R. Keisler, L. Knox, M. Millea, and C. Reichardt, Phys. Rev. D **87**, 083008 (2013).
[9] S. Hannestad, arXiv:0710.1952.
[10] J. Hamann, S. Hannestad, and Y. Y. Y. Wong, J. Cosmol. Astropart. Phys. 11 (2012) 052.
[11] E. Giusarma, M. Corsi, M. Archidiacono, R. de Putter, A. Melchiorri, O. Mena, and S. Pandolfi, Phys. Rev. D **83**, 115023 (2011).
[12] E. Giusarma, M. Archidiacono, R. de Putter, A. Melchiorri, and O. Mena, Phys. Rev. D **85**, 083522 (2012).
[13] J. Hamann, S. Hannestad, G. G. Raffelt, I. Tamborra, and Y. Y. Y. Wong, Nucl. Phys. B, Proc. Suppl. **217**, 72 (2011).
[14] J. Hamann, S. Hannestad, G. G. Raffelt, I. Tamborra, and Y. Y. Y. Wong, J. Phys. Conf. Ser. **375**, 032003 (2012).
[15] G. Mangano, G. Miele, S. Pastor, T. Pinto, O. Pisanti, and P. D. Serpico, Nucl. Phys. **B729**, 221 (2005).
[16] D. J. E. Marsh, E. Macaulay, M. Trebitsch, and P. G. Ferreira, Phys. Rev. D **85**, 103514 (2012).
[17] M. Archidiacono, E. Calabrese, and A. Melchiorri, Phys. Rev. D **84**, 123008 (2011).
[18] M. Archidiacono, E. Giusarma, A. Melchiorri, and O. Mena, Phys. Rev. D **86**, 043509 (2012).
[19] C. L. Bennett *et al.*, arXiv:1212.5225; G. Hinshaw *et al.*, arXiv:1212.5226.
[20] Z. Hou *et al.*, arXiv:1212.6267.
[21] J. Dunkley *et al.*, arXiv:1301.0776; J. L. Sievers *et al.*, arXiv:1301.0824.
[22] J. Dunkley *et al.*, Astrophys. J. **739**, 52 (2011).
[23] The Planck Collaboration, arXiv:astro-ph/0604069.
[24] L. Perotto, J. Lesgourgues, S. Hannestad, H. Tu, and Y. Y. Y. Wong, J. Cosmol. Astropart. Phys. 10 (2006) 013.
[25] J. Hamann, J. Lesgourgues, and G. Mangano, J. Cosmol. Astropart. Phys. 03 (2008) 004.
[26] S. Hannestad, I. Tamborra, and T. Tram, J. Cosmol. Astropart. Phys. 07 (2012) 025.
[27] N. Saviano, A. Mirizzi, O. Pisanti, P. D. Serpico, G. Mangano, and G. Miele, Phys. Rev. D **87**, 073006 (2013).
[28] M. Archidiacono, N. Fornengo, C. Giunti, and A. Melchiorri, Phys. Rev. D **86**, 065028 (2012).
[29] S. Joudaki, K. N. Abazajian, and M. Kaplinghat, Phys. Rev. D **87**, 065003 (2013).
[30] T. D. Jacques, L. M. Krauss, and C. Lunardini, Phys. Rev. D **87**, 083515 (2013).
[31] J. R. Kristiansen and O. Elgaroy, arXiv:1104.0704.
[32] A. Melchiorri, O. Mena, S. Palomares-Ruiz, S. Pascoli, A. Slosar, and M. Sorel, J. Cosmol. Astropart. Phys. 01 (2009) 036.
[33] Planck Collaboration, arXiv:1303.5076.
[34] M. C. Gonzalez-Garcia and M. Maltoni, Phys. Rep. **460**, 1 (2008).
[35] A. Aguilar-Arevalo *et al.* (LSND Collaboration), Phys. Rev. D **64**, 112007 (2001).
[36] B. Armbruster *et al.* (KARMEN Collaboration), Phys. Rev. D **65**, 112001 (2002).
[37] P. Astier *et al.* (NOMAD Collaboration), Phys. Lett. B **570**, 19 (2003).
[38] A. A. Aguilar-Arevalo *et al.* (MiniBooNE Collaboration), Phys. Rev. Lett. **110**, 161801 (2013).
[39] M. Antonello *et al.* (ICARUS Collaboration), Eur. Phys. J. C **73**, 2345 (2013).
[40] M. Martini, M. Ericson, and G. Chanfray, Phys. Rev. D **85**, 093012 (2012).
[41] M. Martini, M. Ericson, and G. Chanfray, Phys. Rev. D **87**, 013009 (2013).
[42] C. Giunti, M. Laveder, Y. F. Li, Q. Y. Liu, and H. W. Long, Phys. Rev. D **86**, 113014 (2012).
[43] G. Mention, M. Fechner, T. Lasserre, T. A. Mueller, D. Lhuillier, M. Cribier, and A. Letourneau, Phys. Rev. D **83**, 073006 (2011).
[44] C. Giunti and M. Laveder, Phys. Rev. C **83**, 065504 (2011).
[45] F. Dydak *et al.*, Phys. Lett. **134B**, 281 (1984).

[46] M. Maltoni and T. Schwetz, Phys. Rev. D **76**, 093005 (2007).
[47] P. Adamson *et al.* (MINOS Collaboration), Phys. Rev. Lett. **107**, 011802 (2011).
[48] K. B. M. Mahn *et al.* (SciBooNE and MiniBooNE Collaborations), Phys. Rev. D **85**, 032007 (2012).
[49] G. Cheng *et al.* (MiniBooNE and SciBooNE Collaborations), Phys. Rev. D **86**, 052009 (2012).
[50] J. M. Conrad, C. M. Ignarra, G. Karagiorgi, M. H. Shaevitz, and J. Spitz, Adv. High Energy Phys. **2013**, 163897 (2013).
[51] K. N. Abazajian *et al.*, arXiv:1204.5379.
[52] A. Lewis and S. Bridle, Phys. Rev. D **66**, 103511 (2002).
[53] B. A. Reid *et al.*, Mon. Not. R. Astron. Soc. **404**, 60 (2010).
[54] L. Anderson *et al.*, Mon. Not. R. Astron. Soc. **428**, 1036 (2012).
[55] N. Padmanabhan, X. Xu, D. J. Eisenstein, R. Scalzo, A. J. Cuesta, K. T. Mehta, and E. Kazin, arXiv:1202.0090.
[56] C. Blake, E. Kazin, F. Beutler, T. Davis, D. Parkinson, S. Brough, M. Colless, C. Contreras *et al.*, Mon. Not. R. Astron. Soc. **418**, 1707 (2011).
[57] A. G. Riess, L. Macri, S. Casertano, H. Lampeitl, H. C. Ferguson, A. V. Filippenko, S. W. Jha, W. Li, and R. Chornock, Astrophys. J. **730**, 119 (2011).
[58] E. Di Valentino, S. Galli, M. Lattanzi, A. Melchiorri, P. Natoli, L. Pagano, and N. Said, arXiv:1301.7343.
[59] E. Calabrese, A. Slosar, A. Melchiorri, G. F. Smoot, and O. Zahn, Phys. Rev. D **77**, 123531 (2008).
[60] M. Archidiacono *et al.* (to be published).